Experimental Study of Multi-cell Counting Based on Inertial Microfluidic Devices.

Author

Muhammad Danish Manshad

Regn Number

00000330460

Supervisor

Dr. Jawad Aslam

Co-Supervisor

Dr Emad Uddin

DEPARTMENT OF MECHANICAL ENGINEERING

SCHOOL OF MECHANICAL & MANUFACTURING ENGINEERING (SMME)

NATIONAL UNIVERSITY OF SCIENCES AND TECHNOLOGY

H-12 ISLAMABAD

January 2023

Experimental Study of Multi-cell Counting Based on Inertial Microfluidic Devices.

Author

MUHAMMAD DANISH MANSHAD

Regn Number

00000330460

A thesis submitted in partial fulfillment of the requirements for the degree of

MS Mechanical Engineering

Thesis Supervisor:

Dr. Jawad Aslam

Thesis Supervisor's Signature:

_____

Thesis Co-Supervisor:

Dr. Emad Uddin

Thesis Co-Supervisor's Signature: _____

DEPARTMENT OF MECHANICAL ENGINEERING

SCHOOL OF MECHANICAL & MANUFACTURING ENGINEERING (SMME)

NATIONAL UNIVERSITY OF SCIENCES AND TECHNOLOGY,

H-12 ISLAMABAD

JANUARY 202

Declaration

I certify that this research work titled "*Experimental Study of Multicell Counting Based on Inertial Microfluidic Devices."* is my own work. The work has not been presented elsewhere for assessment. The material that has been used from other sources it has been properly acknowledged / referred.

Muhammad Danish Manshad
00000330460

Proposed Certificate for Plagiarism

It is certified that MS Thesis Titled "**Experimental Study of Multicell Counting Based on Inertial Microfluidic Devices"** by **Muhammad Danish Manshad** has been examined by us. We undertake the follows:

a. Thesis has significant new work/knowledge as compared already published or are under consideration to be published elsewhere. No sentence, equation, diagram, table, paragraph or section has been copied verbatim from previous work unless it is placed under quotation marks and duly referenced.
b. The work presented is original and own work of the author (i.e. there is no plagiarism). No ideas, processes, results or words of others have been presented as Author own work.
c. There is no fabrication of data or results which have been compiled/analyzed.
d. There is no falsification by manipulating research materials, equipment or processes, or changing or omitting data or results such that the research is not accurately represented in the research record.
e. The thesis has been checked using TURNITIN (copy of originality report attached) and found within limits as per HEC plagiarism Policy and instructions issued from time to time.

Name & Signature of Supervisor

Supervisor Name: **Dr Jawad Aslam**

Signature**:** _____

Signature of Student

Muhammad Danish Manshad

Registration Number (00000330460)

Copyright Statement

Acknowledgements

I am thankful to my Creator Allah Subhana-Watala to have guided me throughout this work at every step and for every new thought which You setup in my mind to improve it. Indeed, I could have done nothing without Your priceless help and guidance. Whosoever helped me throughout the course of my thesis, whether my parents or any other individual was Your will, so indeed none be worthy of praise but You.

I am profusely thankful to my beloved parents who raised me when I was not capable of walking and continued to support me throughout in every department of my life.

I would also like to express special thanks to my supervisor Dr Jawad Aslam and Co supervisor Dr Emad Uddin for their help throughout my thesis and also for the courses which they taught me.

I would also like to pay special thanks to Hassan Sardar for his tremendous support and cooperation. Each time I got stuck in something; he came up with the solution. Without his help I wouldn't have been able to complete my thesis. I appreciate his patience and guidance throughout the whole thesis.

I would also like to thank Dr Adnan Munir, Dr Zeb for being on my thesis guidance and evaluation committee and express my special thanks to Dr Emad for his help. I am also thankful to M Zulfiqar and Khola Ikram for their support and cooperation.

Finally, I would like to express my gratitude to all the individuals who have rendered valuable assistance to my study.

Dedicated to my exceptional parents and adored siblings whose tremendous support and cooperation led me to this wonderful accomplishment.

Abstract

In the field of biomedical, a cell counting device is used for the counting of cells or microparticles for the treatment of different kinds of diseases. The research based on the inertial flow microfluidic focused cell counting. The aim of study is to design and development of a low-cost microfluidic counting device for counting of particles in a focused microchannel. The counting of particles is independent of size, device can be count for different sizes. Using fluorescent microscope and AM Scope the image-based counting has been done at different sized microchannels. Which were fabricated using 3d printed mold and PDMS pouring on the mold. PDMS and Glass slide is bonded using plasma bonding. In the research work, comparison between two scopes have been verified at two different particles solution ratio. The image-based counting has been done by taking videos from the scope's cameras. The particles counting validated by counting the particles using a commercial device Hemocytometer. Results from both the scopes are mainly same, the counting from any of scope can be done and it can be done on mobile phone in future as the results are almost same for both the cases. There were three channel sizes and four different flow rates on which the experiment performed. The experiment performed in a clean room, which shows that the device having least dimension is best for counting microparticles. Also, the counting depends on the flow rate of the solution because increasing the flow rate decrease in total count of microparticles. It can used in lab tests for medical diagnostics, can be portable, easy to use and a low-cost device.

Key Words: *Microfluidics, Cell Counting, Inertial Flow, Multicell, Microchannels*

Table of Contents

List of Figures

List of Tables

CHAPTER 1

INTRODUCTION

1.1 Background, Scope, and Motivation

Cell counting is a fundamental task in many areas of biology and medicine, including cancer research, drug development, and quality control of cell-based products. Traditional cell counting methods, such as the hemocytometer, are labor-intensive and time-consuming, and they often require trained personnel and specialized equipment. In recent years, there has been a growing interest in developing new techniques for cell counting that are more efficient and accurate.

Inertial microfluidic devices have emerged as a promising alternative for cell counting and other applications in biotechnology. These devices use the inertia of fluid flow to manipulate and sort cells, and they have been demonstrated to be effective for a wide range of cell types and sizes. Inertial microfluidic devices have several advantages over traditional methods, including high throughput, low cost, and ease of use.

In this study, we conducted an experimental investigation of multicell counting using inertial microfluidic devices. A microfluidic chip was designed and fabricated with a series of parallel channels and bifurcations, where cells were focused and counted as they passed through the branches. The chip was tested with different cell types and concentrations, and the results were compared with traditional cell counting methods.

1.2 Inertial Microfluidics

Inertial microfluidics is a branch of microfluidics that uses the inertia of a fluid and its contents to manipulate and sort particles or cells within a microfluidic device. This is achieved by designing the microfluidic device to have a series of bends or bifurcations, where the fluid and its contents are forced to follow different trajectories based on their size, shape, and density.

In inertial microfluidic devices, particles or cells are introduced into the device through an inlet and are then directed through a series of microfluidic channels. As they flow through the channels, they

are subjected to a series of bends or bifurcations, which cause them to follow different trajectories based on their inertia. Larger or denser particles or cells will tend to follow a straight path, while smaller or less dense particles or cells will be deflected and follow a curved path.

By carefully designing the geometry and flow rate of the microfluidic channels, it is possible to separate and sort particles or cells based on their size, shape, and density. Inertial microfluidic devices have been used for a wide range of applications, including cell sorting and separation, drug delivery, and microfluidic assays.

One of the main advantages of inertial microfluidics is its simplicity and ease of use. Unlike other methods of particle and cell manipulation, inertial microfluidics does not require the use of external forces or complex control systems, making it relatively easy to implement and operate. In addition, inertial microfluidics is highly scalable and can be used for a wide range of particle and cell sizes and concentrations.

1.3 Focusing

In microfluidics, focusing refers to the process of directing and concentrating fluids or particles into a specific region or location within a microfluidic device. This can be achieved using a variety of techniques, such as hydrodynamic focusing, di-electrophoresis, and inertial focusing.

Hydrodynamic focusing involves using the pressure and flow of a fluid to direct and focus particles or cells into a specific region. This can be achieved by using a series of constrictions and expansions in the microfluidic channel, which cause the fluid and its contents to flow in a particular direction and focus at specific points.

Di-electrophoresis involves using an applied electric field to manipulate and focus particles or cells within a microfluidic device. By applying different electric field gradients, particles or cells can be attracted or repelled, allowing them to be focused at specific locations within the device.

Inertial focusing involves using the inertia of a fluid and its contents to direct and focus particles or cells within a microfluidic device. This can be achieved by using a series of bends or bifurcations in the microfluidic channel, which cause particles or cells with different sizes and densities to follow different trajectories and focus at specific locations within the device.

Overall, the process of focusing in microfluidics is important for a variety of applications, including cell sorting and separation, drug delivery, and microfluidic assays.

The process of focusing particles or cells within a microfluidic device can depend on the flow rate of the fluid. In general, increasing the flow rate can lead to a more focused stream of particles or cells, while decreasing the flow rate can lead to a less focused stream.

For example, in a microfluidic device with a series of bends or bifurcations, increasing the flow rate can cause the particles or cells to follow a more predictable and focused trajectory through the device. This is because the increased flow rate provides more inertia to the particles or cells, causing them to follow a more straight path through the bends and bifurcations.

On the other hand, decreasing the flow rate can cause the particles or cells to follow a less predictable and focused trajectory through the device. This is because the decreased flow rate provides less inertia to the particles or cells, causing them to follow a more curved path through the bends and bifurcations.

Overall, the flow rate can have a significant effect on the focusing of particles or cells within a microfluidic device, and it is important to carefully control the flow rate in order to achieve the desired focusing results.

1.4 Methods For Fabricating

There are several methods for fabricating microfluidic chips, which can be classified into two main categories: top-down and bottom-up approaches.

1.4.1 Top-Down Approaches

Top-down approaches involve the direct machining or etching of microfluidic channels and structures into a substrate material, such as glass or silicon. These approaches include photolithography, which uses light-sensitive resists and etching to pattern the substrate; laser ablation, which uses a laser beam to vaporize material from the substrate; and milling, which uses a rotary tool to cut the channels into the substrate.

1.4.2 Bottom-Up Approaches

Bottom-up approaches involve the assembly of microfluidic devices from smaller units or building blocks. These approaches include the use of microfluidic "inks," which are viscous fluids containing particles or other materials that can be printed or drawn into desired patterns; self-assembly, which

relies on the natural forces of attraction or repulsion between particles or molecules to spontaneously form structures; and microinjection molding, which uses a mold to shape molten polymer into the desired microfluidic structure.

There are also hybrid approaches that combine elements of both top-down and bottom-up fabrication methods. For example, microscale 3D printing techniques can be used to build up microfluidic structures layer by layer, combining the precision of photolithography with the flexibility of "inks" or other materials.

In general, the choice of fabrication method for microfluidic chips depends on the specific requirements and constraints of the application, such as the materials used, the size and complexity of the structures, and the desired production volume.

1.4.3 Rapid Prototyping

Rapid prototyping is a process of quickly creating a physical model of a design or concept using additive manufacturing or other rapid prototyping technologies. This allows designers and engineers to quickly test and iterate on their ideas, without the need for costly and time-consuming traditional manufacturing processes.

There are several types of rapid prototyping technologies, including:

- 3D printing: This involves creating a physical model by depositing layers of material, such as plastic or metal, in a predetermined pattern.
- CNC machining: This involves using computer-controlled cutting tools to remove material from a block of material to create the desired shape.
- Vacuum casting: This involves creating a mold of the prototype using a silicone rubber mold, and then casting the prototype using a liquid resin.

Rapid prototyping allows designers and engineers to quickly create physical models of their designs and test them in real-world conditions, which can save time and money in the development process.

CHAPTER 2

LITERATURE REVIEW

Most of the developing countries, number of deaths occurred due to the unavailability of medical diagnostics and treatment[1]. Microfluidic devices extensively used in the biomedical applications such as cell counting, cell segregation[2]. Diseases such as rise in white blood cells due to physiological (Newborn, delivery, pregnancy) and Pathological (Leukemia, bacterial inflammation, uremia) conditions and decline in white blood cells due to malaria, viral infection, typhoid etc. are common diseases[3]. Microfluidics consist of channels or microchips having dimensions approximately hundreds of micrometers and deals with fluid flow which is precisely controlled[4]. The advantages of microfluidics include, but are not limited to, the usage of smaller amounts of samples and reagents, quick sample processing, high sensitivity, low cost, enhanced portability and the ability to be highly integrated and automated, minimizing human error and intervention[5].

2.1 Impedance Based Counting

Several methods have been discovered for the cell counting such as impedance-based counting, cells are detected using electrical signals when they passed from the sensing electrode based on changing impedance of the system[6]–[15]. Seto, Hirokazu et al. using for counting microparticles named as metal mesh device, only mesh sized particles were counting correctly, smaller particles passed from the mesh[16], [17]. Lin Y et al. introduced the optical detection, counting and separation of microparticles using the Di-electrophoretic forces[18], [19]. Strohm et al. proposed a cell counting technique in which acoustic waves used to count cells as ultrasound beam scattered by the cells, the spectral details gave the sign of detection[20]. Zachary J. Smith et al. used an image-based technique for counting cell, sample passed using capillary action through sensing chamber[21].

Focusing plays a vital role in counting cells in flow cytometry[22]. Focusing can be done using different methods such as sheath flow, dielectrophoretic, elasto-inertial based microfluidic focusing, shape depended focusing technique.[23]–[28]

These methods may provide more precise detection results, but equipment and device manufacturing techniques are very expensive and took hours for fabrication a chip, bulky, and extensive training required for operators greatly restrict their use[29].

In this work, an image-based multi size microparticles counting method is presented using an inertial microfluidic device with a curvature to create centrifugal force on microparticles for the purpose of focusing them on a streamline or equilibrium position[30]. This device provides an approximate counting method similar to commercially available devices. The microfluidics devices were tested under different flow rates with varying channel dimensions.

2.2 Image-Based Techniques

There has been a significant amount of research on image-based techniques for counting microcells or microparticles. These techniques often involve the use of microscopes or other imaging systems to visualize and analyze the microcells or microparticles.

One popular image-based counting technique is brightfield microscopy, which utilizes transmitted light to visualize samples. This technique is commonly used for the counting of cells or particles in aqueous samples but may not be suitable for transparent or highly refractive particles.

Another image-based counting technique is phase contrast microscopy, which utilizes the difference in refractive index between a sample and its surroundings to visualize the sample. This technique is often used for the counting of cells or particles in aqueous samples and can be more sensitive than brightfield microscopy for the detection of transparent or highly refractive particles.

Fluorescence microscopy is another image-based counting technique that utilizes fluorescent dyes or markers to visualize cells or particles. This technique is often used for the counting of specific cell types or subpopulations and can provide high sensitivity and specificity.

Overall, image-based counting techniques provide a wide range of options for the analysis of microcells or microparticles, with each technique offering its own advantages and limitations.

2.3 ImageJ

ImageJ is a popular image processing software developed by the National Institutes of Health (NIH). It is widely used in the fields of biology, medicine, and materials science for the analysis and visualization of images.

One of the main strengths of ImageJ is its versatility, as it can be used to analyze a wide range of image types, including microscopy images, medical images, and satellite images. It has a user-friendly interface and a large number of built-in functions for tasks such as image processing, analysis, and visualization.

In addition to its built-in functions, ImageJ also has a large and active community of users who have developed and shared a wide range of plugins and macros to extend its capabilities. This has made

ImageJ a popular choice for researchers who need to perform specialized or customized image analyses.

Overall, ImageJ is a powerful and widely used image processing software that is well-suited for a variety of image analysis tasks.

ImageJ is a popular image processing software that can be used for image-based counting of microparticles or microcells. Here is a general workflow for counting microparticles or microcells using ImageJ:

- Acquire images of the sample using a microscope or other imaging system.
- Import the images into ImageJ.
- Pre-process the images as needed, such as adjusting brightness and contrast or applying filters to enhance the visibility of the particles.
- Use the "Threshold" function in ImageJ to convert the image to a binary image, where the particles are white, and the background is black.
- Use the "Analyze Particles" function to automatically detect and count the particles in the image. This function allows you to set size and shape parameters to exclude larger or smaller objects from the analysis.
- Review the counted particles and adjust the analysis parameters as needed to optimize the accuracy of the count.
- Save the counted particle data for further analysis or reporting.

Overall, ImageJ provides a powerful and user-friendly platform for image-based counting of microparticles or microcells.

CHAPTER 3

MANUFACTURING METHODOLOGY

3.1 Fabrication of Microchannels

The fabrication of microchannels is commonly achieved through the use of the "mold replica" or soft lithography method. A mold is created using a 3D printer, such as the Form 3 or Form lab SLA 3D printer[31].

3.1.1 Mold Fabrication

- 3D model of microchannel is modeled in SolidWorks, having the dimensions equal to the available glass slides.

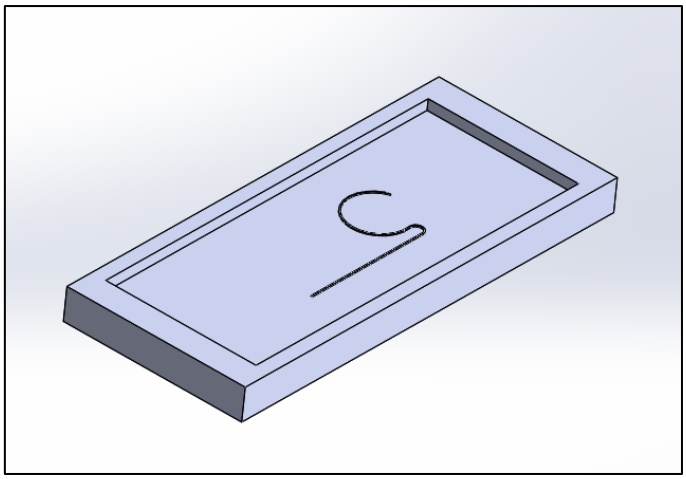

Figure 1 Mold 3D Model

- STL file from the Solidworks imported to the Preform 3D printer software to set for printing.

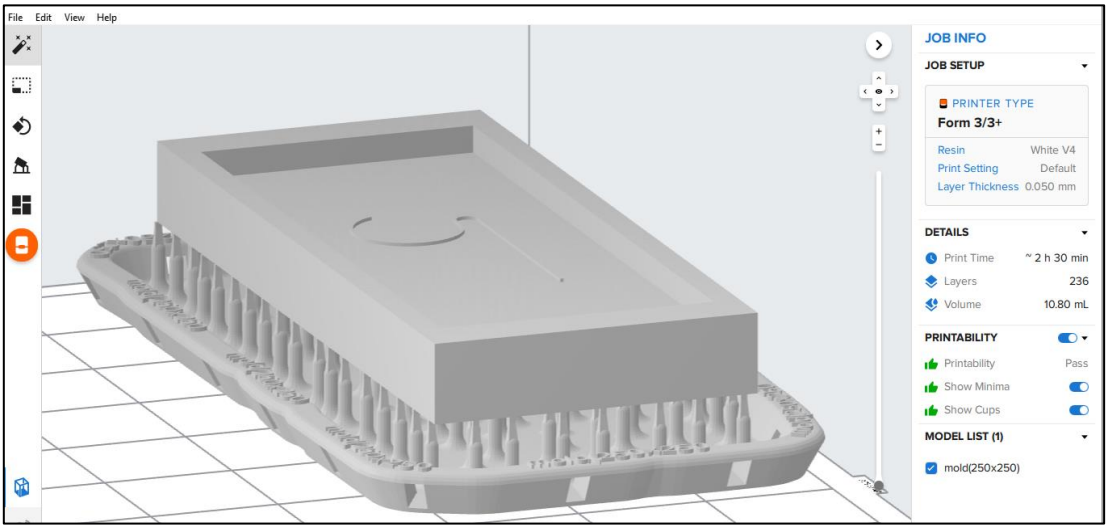

Figure 2 PreForm Setting

- After setting in preform then Form Labs 3 Form 3D printer starts printing after printing commands

Figure 3 3D Printing on Form Labs 3D Printer

- After printing first the 3D printed mold wash in form Wash in Isopropyle Alcohol (IPA) for dissolving the extra resin from the printed part. And the in Form cure the part is cured for 30 minutes at 60 degrees celcius.

Figure 4 Form Labs 3D Printer, Form Cure, Form Wash

- After curing, the final mold with channel pattern on it is fabricated as shown below.

Figure 5 3D Printed Final Mold

3.1.2 PDMS Preparation Procedure

- First Silicon Elastomer and curing agent measured in the ratio of 10:1 using the measuring balance.
- Degas for 30 minutes in desiccator to remove bubbles from the Elastomer mixture.

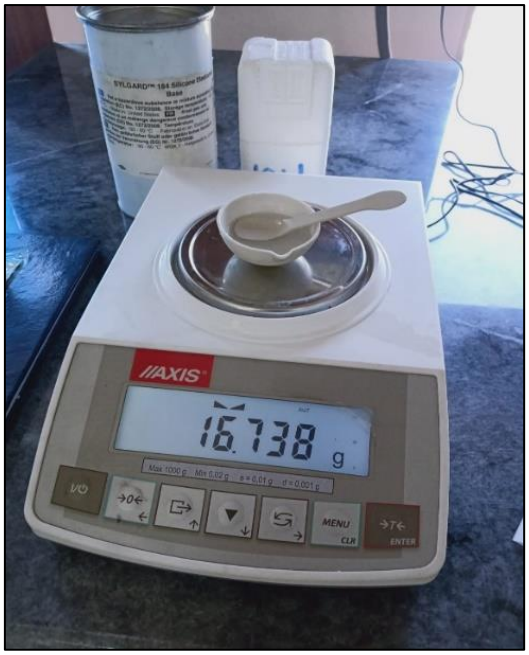

Figure 6 Weighing Scale

- After removing bubbles from the liquid elastomer, pouring into the mold and again degas for removing bubbles from the liquid.

Figure 7 Desiccator

- The liquid elastomer put in Thermostat Oven for soft baking. It took almost 2 hours at 80 degrees Celsius.
- After baking the next step is to peel off the channel from the mold using cutter.

Figure 8 Thermostat Oven for soft baking

- First cut sides and using edge of cutter pull out the PDMS from the mold.

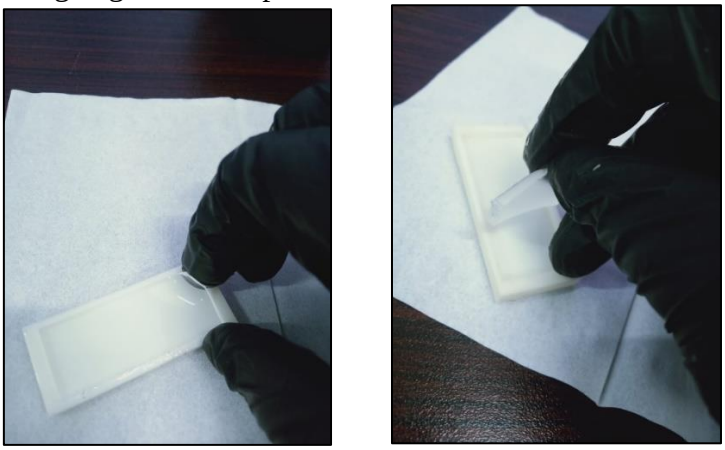

Figure 9 Peeling Off

- Next step is to create holes for inlet and outlet using Biopsy Punch of 2mm diameter.

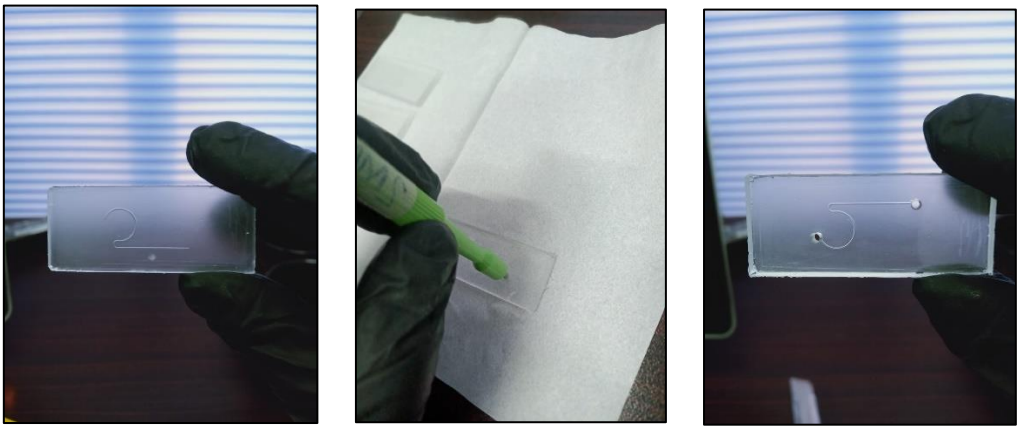

Figure 10 Punching Holes into Microchannel

- After punching holes, next task is to bond the channel with microscope glass slide, which is done by using Plasma Vent, also called plasma bonding.
- After bonding press channel gently to ensure the bonding of PDMS with Glass slide.

- At Last, when bonding is done, soft bake for 10 minutes for making bond stronger.
- To check the bond, leakage test with colored ink solution passed from the final channel which gives satisfactory results for the wide range of flow rate.
- Three different dimension channels fabricated using these above all steps.
- Final channels are show below in the figure.

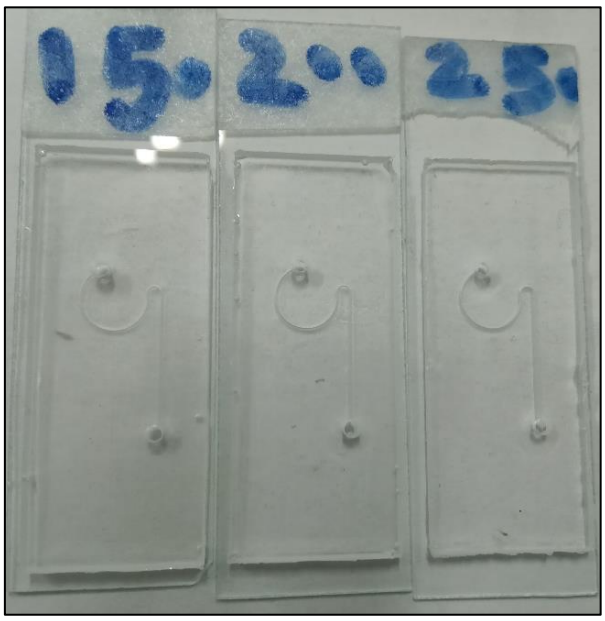

Figure 11 Final Channels

Figure 12 Microchannel comparison with coin

3.1.3 Mold Preparation Flow Chart

Figure 13 Mold Preparation

3.1.4 Mold Preparation flow chart

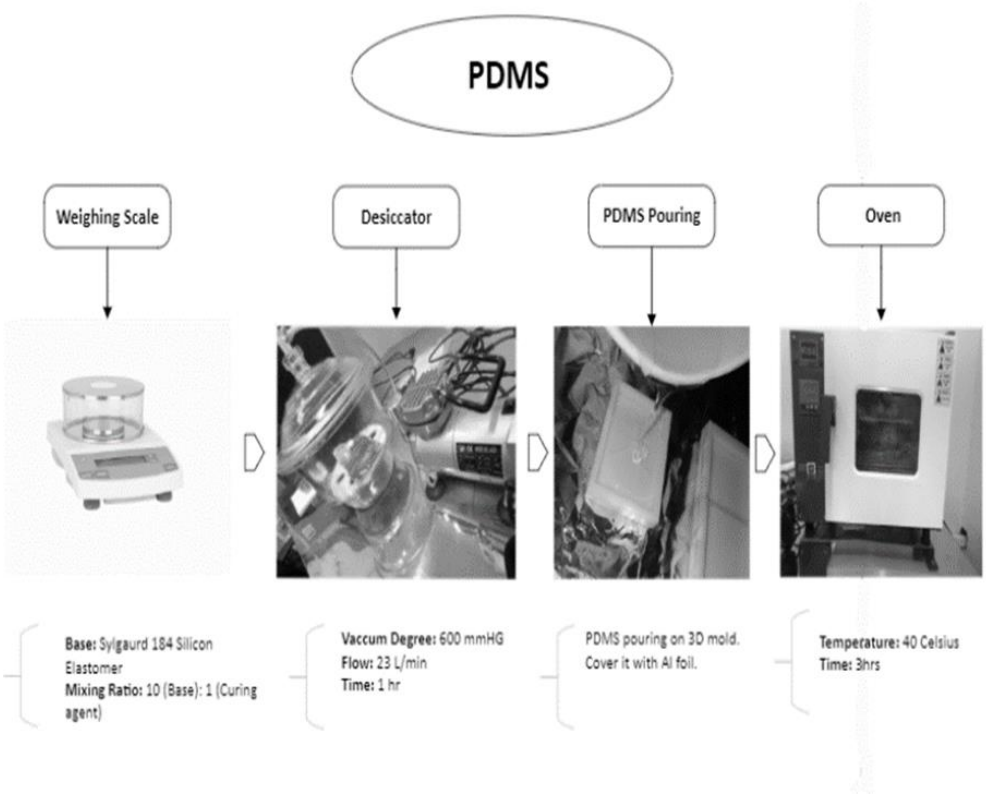

Figure 14 PDMS Preparation

3.1.5 Final steps or postprocessing

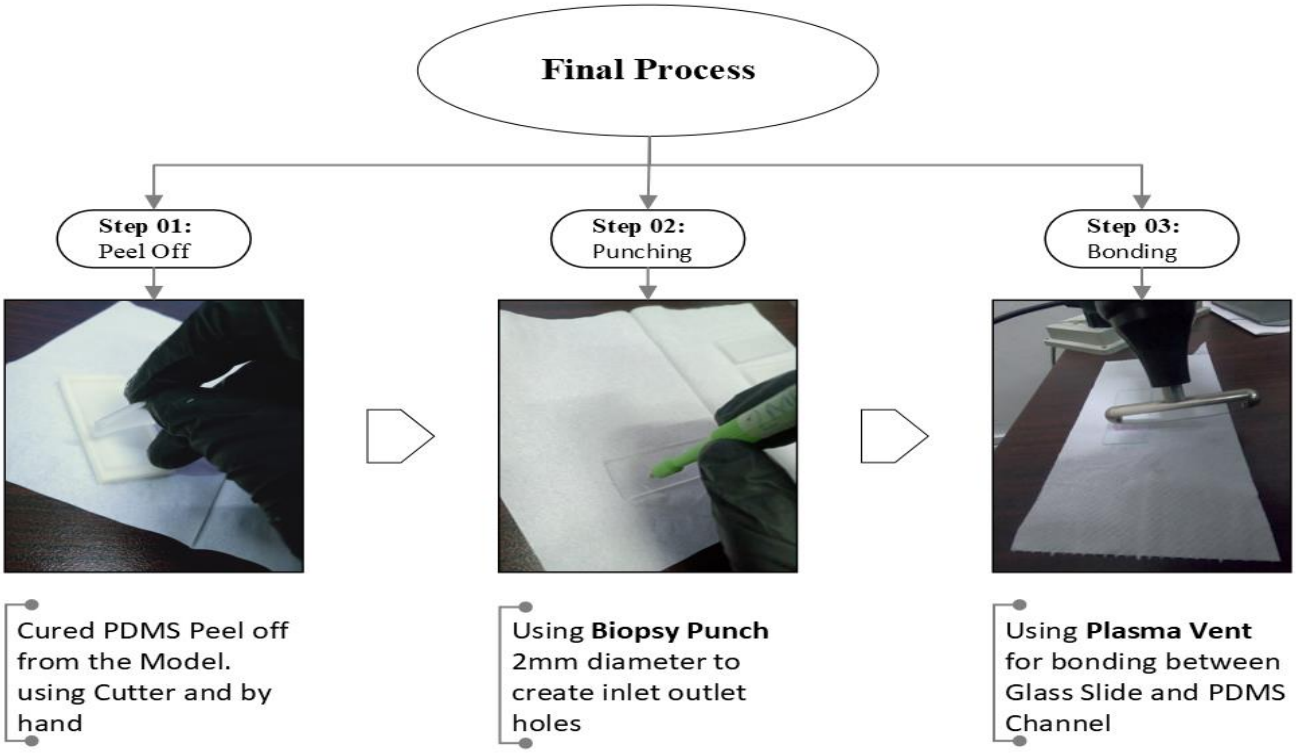

Figure 15 Final Steps

CHAPTER 4

EXPERIMENTATION

4.1 Overview of Experimentation

The experiment was conducted to study the effect of various variables such as channel size, flow rates, and capturing devices. Three different sized channels were fabricated (150µm x 150µm, 200µm x 200µm, 250µm x 250µm). Fluid flow rates of 1µL/min, 5 µL/min, 10 µL/min and 15 µL/min were used. The flow was captured using two different scopes: an AM Scope with a 40x lens and an XDY-2 Inverted Fluorescent Microscope with a 10x lens magnification. The particles were flowing in two different ratios, representing normal and abnormal conditions for blood cells. This research studies cell counting on microchips at different flow rates and also compares the use of two different types of scopes.

4.2 Design of Experiment

Flow Rates:1, 5, 10, 15 (µL/mint)

Particle Ratios: Normal, Infectious, Dosed

- Normal Ratio (RBC=5100, WBC= 7.75, P=275) x10E9/L (Average Values)
  (RBC: WBC:P = 1: 0.0015: 0.05)
- Infectious Ratio (RBC=5100, WBC= 27.5, P=275) x10E9/L (Average Values)
  (RBC: WBC:P = 1: 0.005: 0.05)
- Dosed Ratio (RBC=5100, WBC=12.09, P=275) x10E9/L (Average Values)
  (RBC: WBC:P = 1: 0.002: 0.05)

Difference between infectious and dosed is very small so, only two types of concentration will be considered. i.e., Normal, and infectious

Channel Size: 150, 200, 250 microns

Particle size: 9, 15 microns

Total cases 6 x 4 = 24 for only 1 method

So, Total cases for 3 methods = 24*2 = 48

Table 1 Design Parameters

Sr. No	Test Parameters	Description
1	Channel Size(micron)	150, 200, 250
2	Particle's Concentration (%)	(R1=90%-10%), (R2=60%-40%)
3	Flow rates (µL/min)	1, 5, 10, 15
4	Test Equipment	AM Scope, Fluorescent Scope

4.3 Working Fluid Preparation

Sample preparation was done by matching the viscosity of blood using a mixture of 80% water (Deionized Water) and 20% glycerin to make the working fluid more viscous[32]. Microparticles with diameters of 9 microns and 15 microns were added by measuring 0.0125g of mass in a specific ratio. In the first case, the ratio was 1, which consisted of 90% of 9-micron particles by mass and 10% of 15-micron particles. This represents the normal condition, as red blood cells are typically much more prevalent than white blood cells. In the second ratio, the 9-micron particles made up 60% of the mass and the 15-micron particles made up 40%, resulting in a total mass of 0.0125g. This ratio represents an abnormal condition where the number of cells deviates from the normal range. The mixture was then sonicated in an ultrasonicator for 10 minutes to form a uniform and homogenous mixture.

Table 2 Working Fluid Preparation

Sr#	% Concentration of mixture	Quantity
1	Mixture total volume	2 ml
2	Syringe total Volume	1 ml
3	Distilled water % volume	80%
4	Glycerin % volume	20%
5	Particle mass (9&15 micron)	0.125g

4.4 Experimental Setup

The experiment was conducted in a clean room. The working fluid was pumped through the microfluidic chip using a syringe pump (Darwin Microfluidic Pump). A 1-ml syringe filled with the

working fluid containing the mixture of particles was passed through the microchannel by adjusting the flow rate from the syringe pump. The flow from the chip was observed through a vertical microscope equipped with a camera (BioCam Microscopy BIC-E3S-1.5C, 1.5MP) and connected to a computer or laptop to record the fluid flow from the microchip. The tubes used for fluid flow were connected to the inlet and outlet and directed to a petri dish.

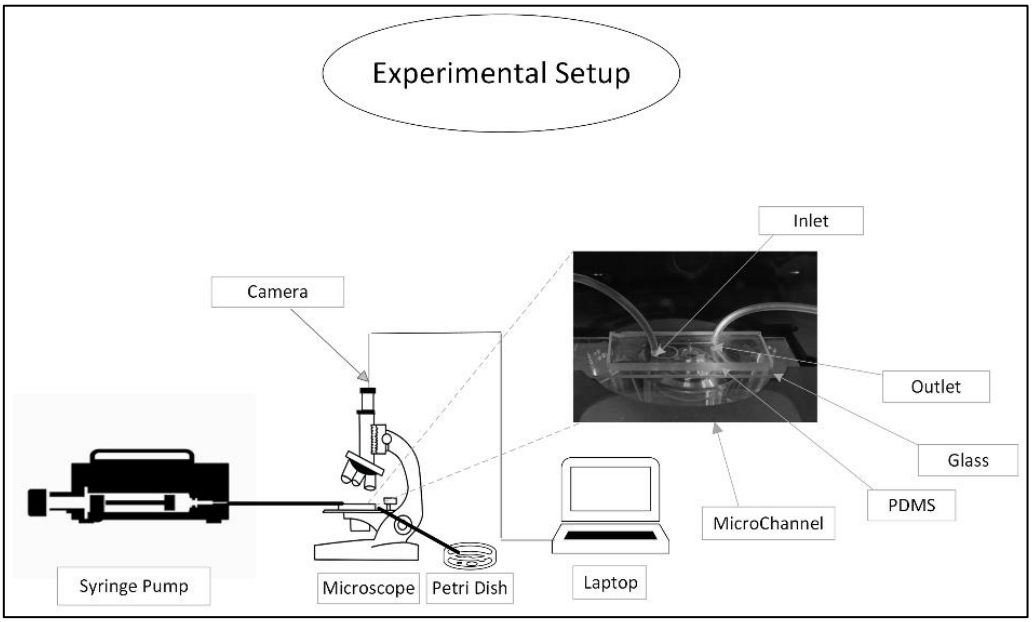

Figure 16 Experimental setup

4.4.1 Syringe Pump Calibration

Set different flow rates, by noting time using stopwatch and note down to volume which displaced by the pump. Using formula q = v/t, find the time taking to displace 0.1mL volume with 0.3mL/hr flow rate. Both the time was exactly same.

Figure 17 Syringe Pump

4.5 Microscopes

In this experimentation, two different capturing devices used for the recording videos. The first one is AM scope and second one is XDY-2 fluorescent scope. In AM scope the lens 40x is used because micron particles and micron channel well focused in 40x. but in comparison with XDY-2 fluorescent scope, the lens used for capturing microparticles is 10x. because XDY-2 fluorescent scope have higher resolution then the AM scope. Both scopes are equipped with cameras.

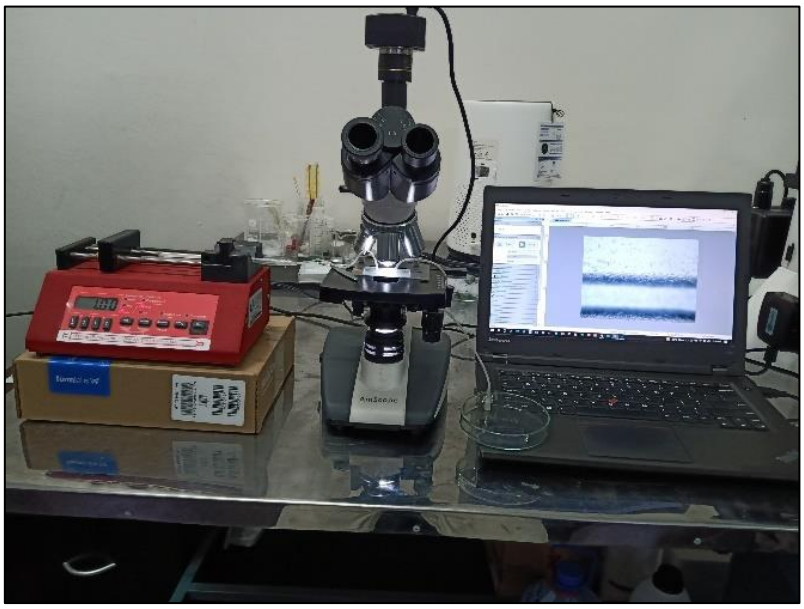

Figure 18 Experimental Setup in the Lab(AM Scope)

Both cameras having 30 fps capturing abilities. After passing working fluid from the microchannel the videos which consist of 2 minutes has been captured for further processing

Figure 19 Experimental Setup in the Lab (Fluorescent Scope)

4.5.1 Microscope Calibration

Calibrating a microscope is the process of adjusting and verifying the accuracy and precision of the instrument's measurement and display scales. This is important because the accuracy of the measurements made using a microscope can be affected by various factors, such as the quality of the optics and the stability of the stage.

There are several methods for calibrating a microscope, including:

- Objective lens calibration: This involves verifying the accuracy of the objective lens magnification by comparing it to a known reference, such as a stage micrometer.
- Stage micrometer calibration: This involves verifying the accuracy of the stage micrometer by comparing it to a known reference, such as a calibrated eyepiece graticule.
- Eyepiece graticule calibration: This involves verifying the accuracy of the eyepiece graticule by comparing it to a known reference, such as a stage micrometer.

It is important to regularly calibrate a microscope to ensure the accuracy of measurements made using the instrument. Calibration procedures may vary depending on the specific microscope model and should be performed according to the manufacturer's recommendations.

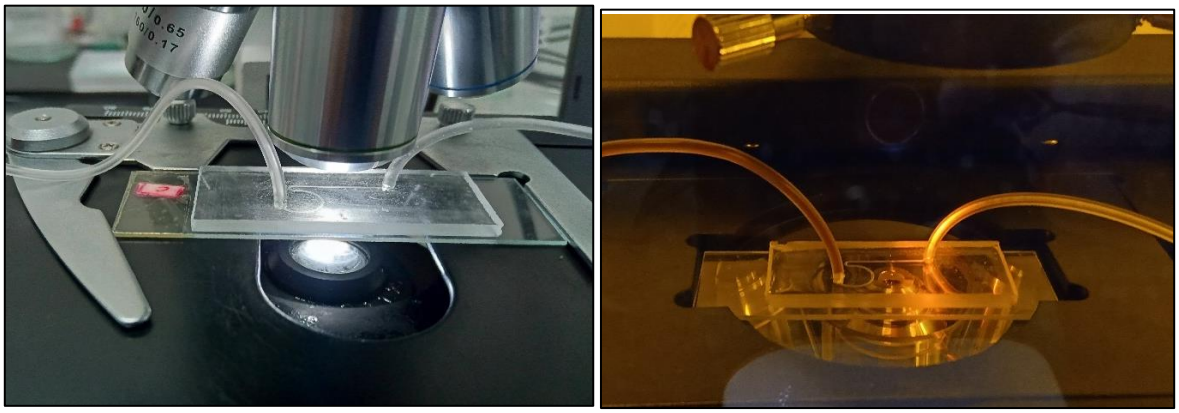

Figure 20 Microchannel under both microscopes a) AM Scope b) Fluorescent Scope

4.6 Counting Technique

The experiment was conducted by recording the fluid flow from the microchannel using a microscope camera. The videos were then converted into frames at different flow rates and the frames were converted into grayscale images. The post-processing was done using the ImageJ software to count the particles in the desired frame. The process started with enhancing the visibility of the image by adjusting the brightness and contrast. The length and width of the frame were calibrated in ImageJ according to the scope's magnification. A threshold was set to remove any unnecessary noise from the

image, and it was converted into a binary image in which the background was removed and the microparticles were highlighted. In the final step, the particles were analyzed, and ImageJ counted the particles according to the area of the particles and provided the results in a spreadsheet with the total count.

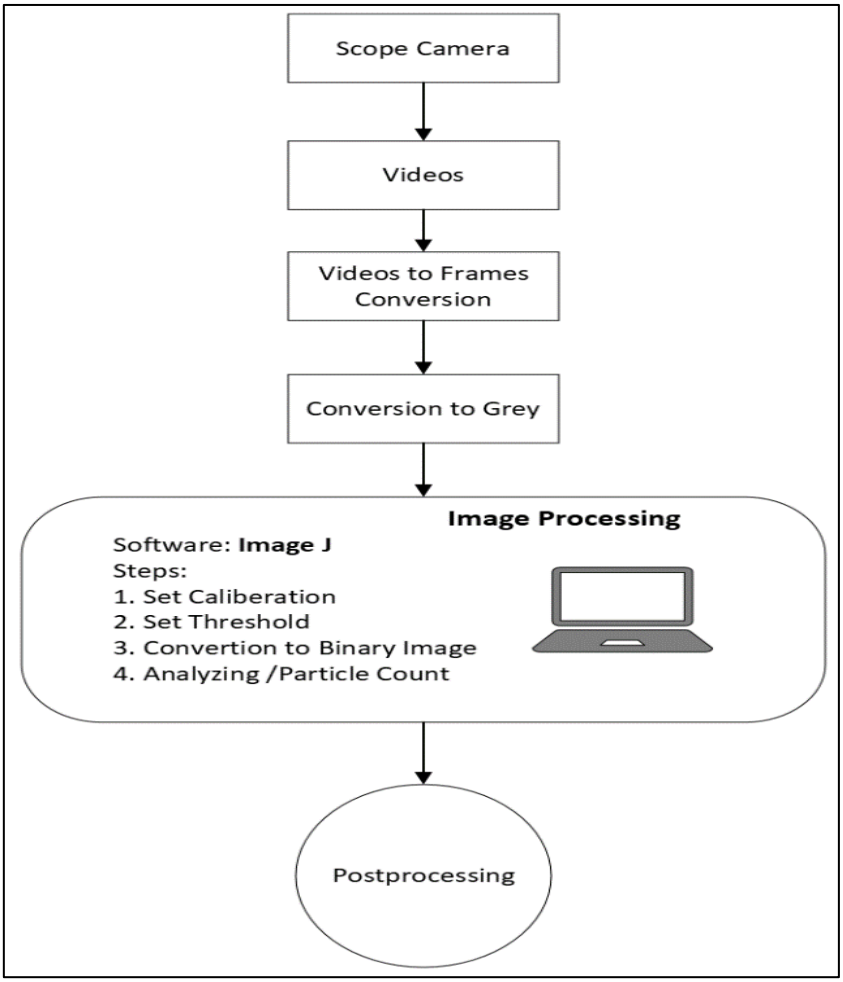

Figure 21 Counting technique flow chart.

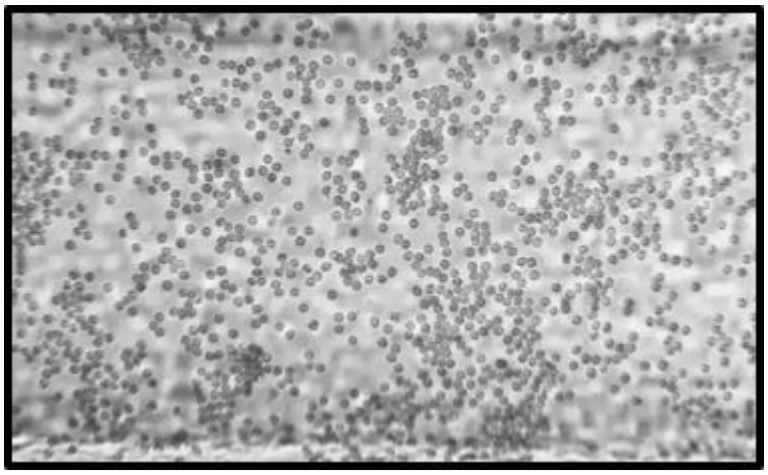

Figure 22 Grey Image Input

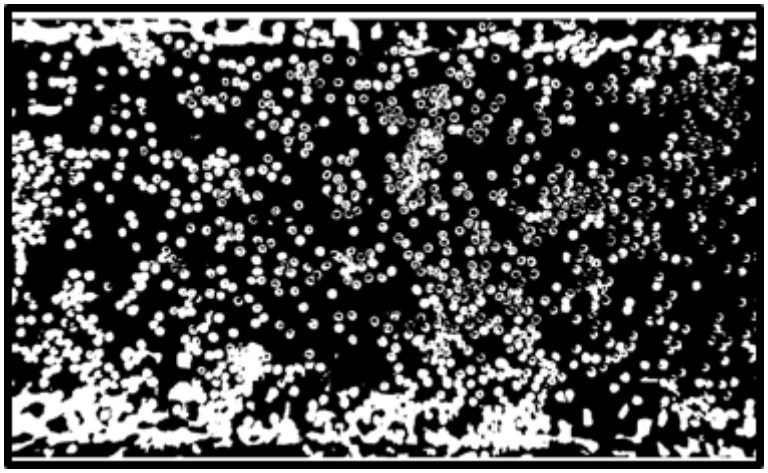

Figure 23 Binary Image

In Binary image, the grey scaled image converted into black and white image in which the particles are in in white color whereas the background removed and shown a black color. The watershed option in ImageJ creates the particles sperate if the particles are coagulated or in clustered form. The final image consists of particles with outlined with red circle around them. The ImageJ software gives the excel sheet of the results in form of area mentioned of each particle in the image. From the area using circle formula convert into the diameter which is post processed.

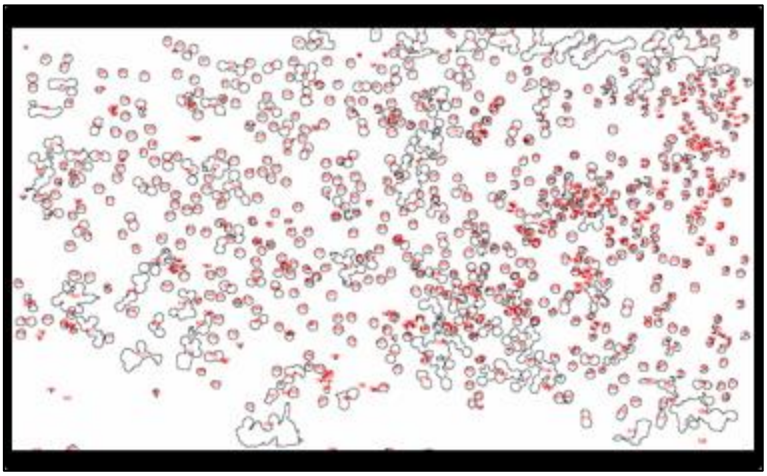

Figure 24 and Counted image Output.

CHAPTER 5

RESULTS AND DISCUSSION

5.1 Results Validation

The graph below shows the validation of ImageJ counting technique. The ImageJ technique is compared with the manual counting which is down using the Hemocytometer. Hemocytometer is a device which is used to count microcells, in which the volume and dilution factor is known. By using the dilution factor and total count in the chamber of hemocytometer, convert into the per milli litter, which represent the total count. As graph shown below which shows that the count from the ImageJ and the hemocytometer is almost same. There is only 1.71% error in 9-micron particles and 1.2% error in 15-micron particles. This validate that the counting technique can be used for the further study.

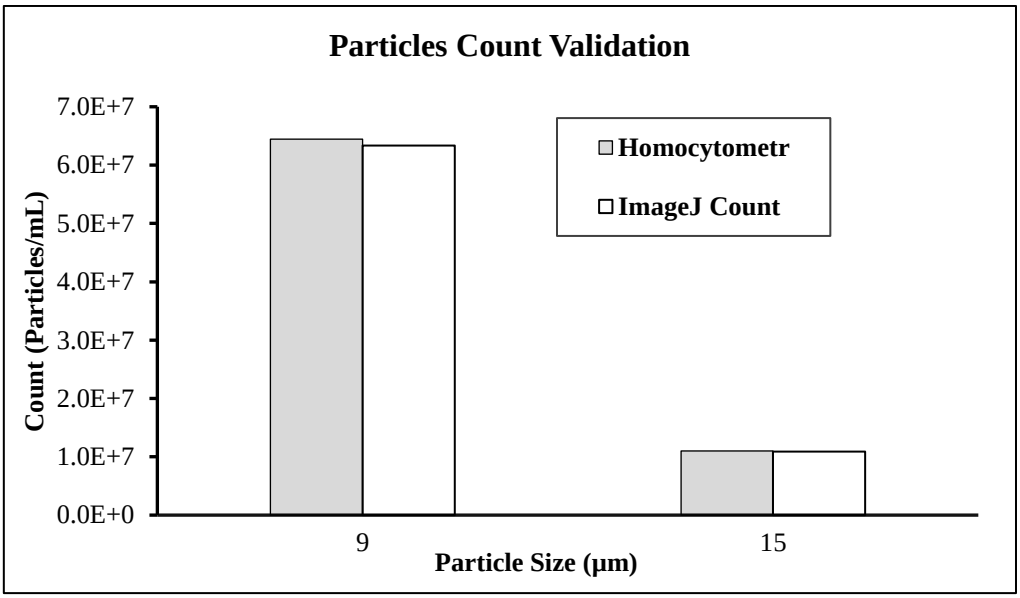

Figure 25 Validation Graph

5.2 Counting Results

The particle counting was done and presented separately according to the size of the particles and the ratio of the particles. The graphs show the results for ratio one, in which the 9µm particles are 90% and the 15µm microparticles are only 10%. The dotted line shows the reference count of particles in each graph (6.45E07 Cells/mL for 9µm particles and 1.10E07 Cells/mL for 15µm particles). The reference counting was done using a commercial device known as a Hemocytometer. The counting technique results were first compared with the commercial counting device and then experiments were

performed at different flow rates. The comparison study presents the results from both scopes. The trend in the graphs in each case is almost the same, as the flow rate increases, the total cell count decreases. Also, it has been observed that the wider the channel, the lesser the total count.

a) b)

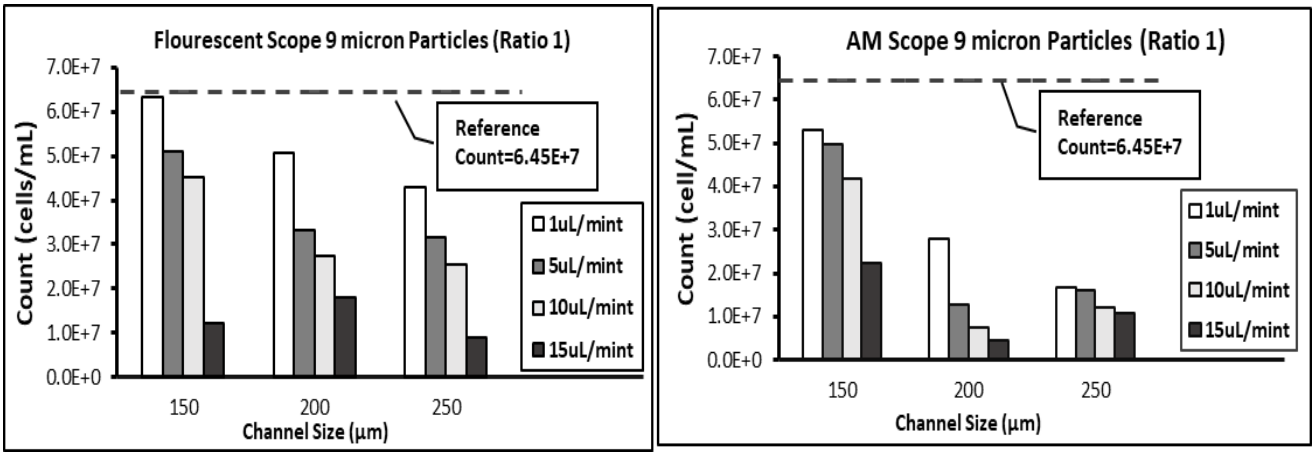

Figure 26 a) graph between the total count vs channel dimensions at different flow rates, the results of XDY-2 fluorescent scope having particle size 9µm. b) The results from the AM scope of ratio-1 having particle size 9µm.

c) d)

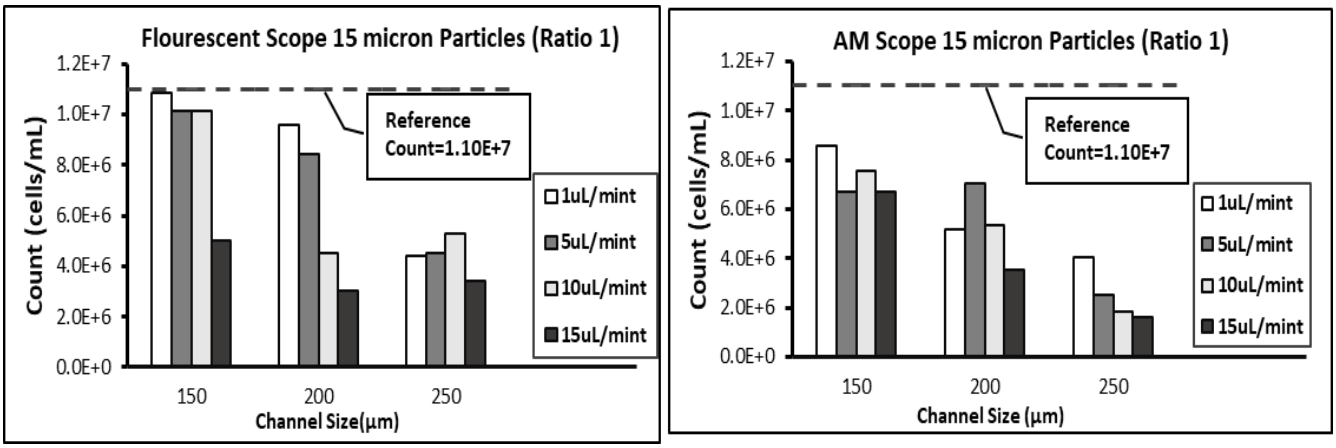

Figure 27 c) The results from XDY-2 fluorescent scope of ratio-1 having particle size 15µm d) The results from the AM scope of ratio-1 having particle size 15µm.

The experiment was also performed on an abnormal condition where the blood count is distorted from the normal range by changing the ratio of particles. As any abnormality happens, the ratio of cells is also disturbed. To capture and count the different number of microparticles under abnormal conditions, we ensured that the chip can also work for abnormal conditions. The graph shows that the reference values also change from the previous one because the ratio is changed, as the 9µm particles are 60% and the 15µm microparticles are only 40%. But the trends are the same, where the 1µL/min gives the highest/nearest count to the reference value. As the flow rate increases to 15µL/min, the count is much

lower. In all cases, the geometry having 150µm x 150 µm has the maximum output. Where 250µm is less efficient in comparison to the other devices.

a) b)

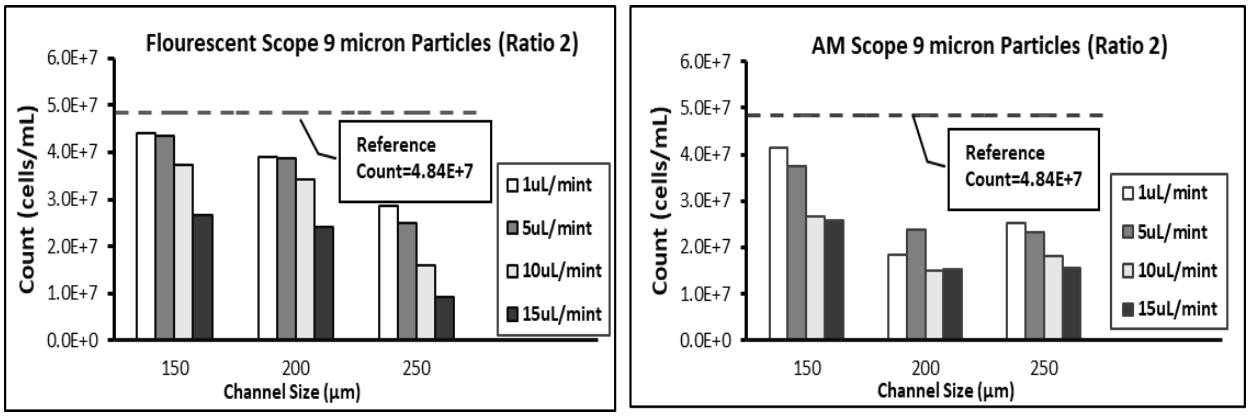

Figure 28 a) Graph between the total count vs channel dimensions at different flow rates, the results of XDY-2 fluorescent scope having particle size 9µm. b) The results from the AM scope of ratio-2 having particle size 9µm.

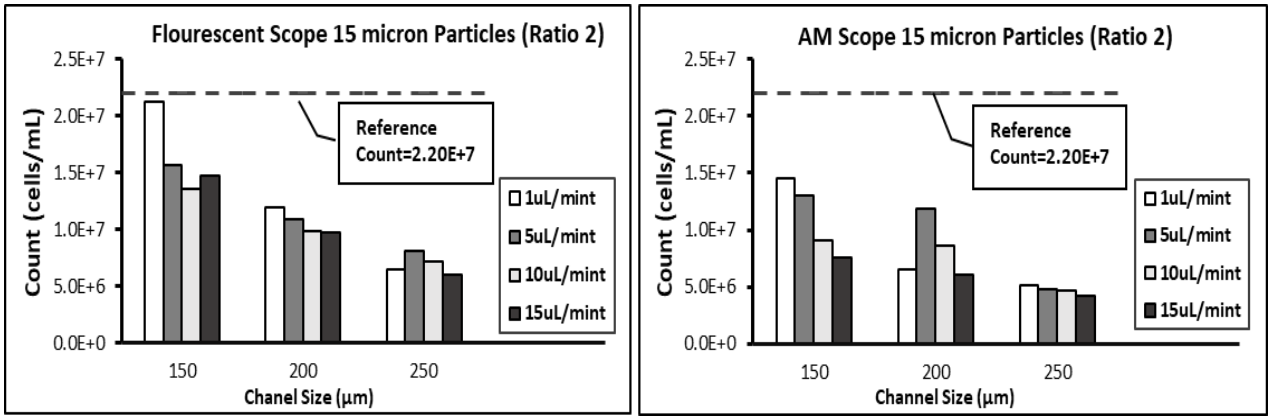

Figure 29 c) The results from XDY-2 fluorescent scope of ratio-1 having particle size 15µm d) The results from the AM scope of ratio-2 having particle size 15µm.

5.2.1 Why Results Deviate

The reason for the lower count in the final counting is that as the channel becomes wider, the focused region by the lens becomes smaller, causing the corner edges to become blurred during the capturing of images and videos. When unclear images are imported into ImageJ, they are not considered as cells or particles at the edges of the channels.

The figure shows that the grayscale image is blurred in the highlighted corner regions and after converting it into binary, the image cannot differentiate the particles at the corners. That's why in the final image count, ImageJ does not consider the portion that is blurred. As a result, particles are missing from these regions, as shown in the figure.

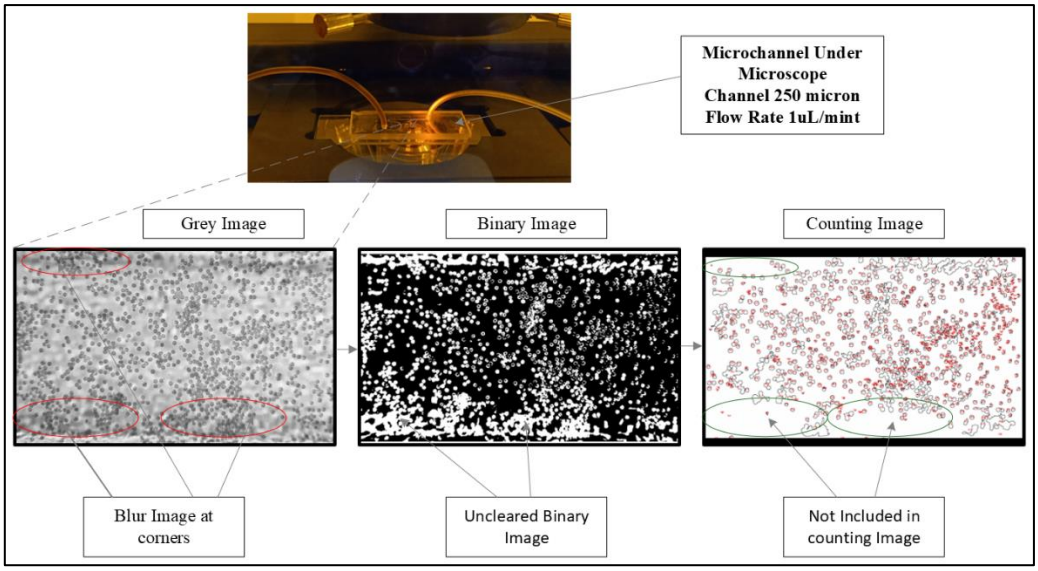

Figure 30 Channel 250µm having flow rate of 1µL/mint.

The results as from the above graphs, it is concluded that the microchannel having least dimension which s 150 micron is best for the counting at 1µL/mint of flow rate. The table below shows the percentage error in 150-micron channel at different flow rates. As from the table the percentage error during flow rate of 1µL/mint is only 1.7% when particles are 9 micron and 1.3% in 15-micron particles. It has been seen that the error percentage decreases as the particles sizes increases but as flow rate increases the error percentage also increases. Because faster the flow capturing ability of the cameras are low, as camera has only 30 frames per second.

Table 3 Error Percentage

Sr #	**Channel Size (micron)**	**Flow Rate (µL/min)**	**% Error Particle 01 (9micron)**	**% Error Particle 02 (15micron)**
1	**150**	**1**	**1.7%**	**1.3%**
2	150	5	20.6%	7.8%
3	150	10	29.9%	17.8%
4	150	15	31.0%	24.3%

The focusing of particles in a microfluidic chip is achieved through the use of inertial forces. Inertial forces are the forces that act on a particle as it moves through a fluid. In a microfluidic chip, particles are typically focused by creating a flow pattern that generates a centrifugal force on the particles. The

centrifugal force causes the particles to move to the outer edges of the channel, where they can be concentrated and separated.

5.3 Focusing Results

The focusing of particles in a microfluidic chip also depends on various factors such as particle size, shape, density, and viscosity of the fluid. For example, larger particles are more difficult to focus due to their inertia, while smaller particles can be focused more easily. The shape of the particles also plays a role in focusing, as particles with a round shape are more easily focused than particles with an irregular shape.

Another important factor that affects the focusing of particles in a microfluidic chip is the channel geometry. The channel geometry can be designed to create specific flow patterns that enhance the focusing of particles. For example, channels with a constriction in the middle can be used to create a flow pattern that generates a higher centrifugal force on the particles, resulting in better focusing.

Additionally, the flow rate is an important factor which can change the focusing. As the flow rate increases, the particles are less focused because the dynamic forces on the particle are less. So, the flow rate should be optimized for the best focusing.

In summary, the focusing of particles in a microfluidic chip is achieved by utilizing the inertial forces generated by the fluid flow pattern in the chip, which is influenced by various factors such as particle size, shape, density, viscosity of the fluid, channel geometry and flow rate.

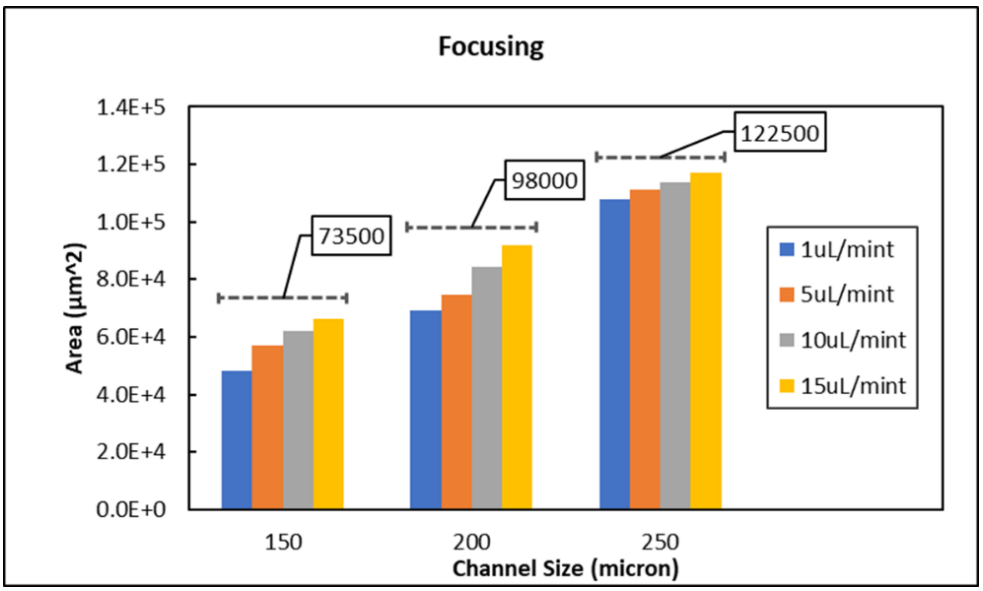

Figure 31 Focusing in all channels.

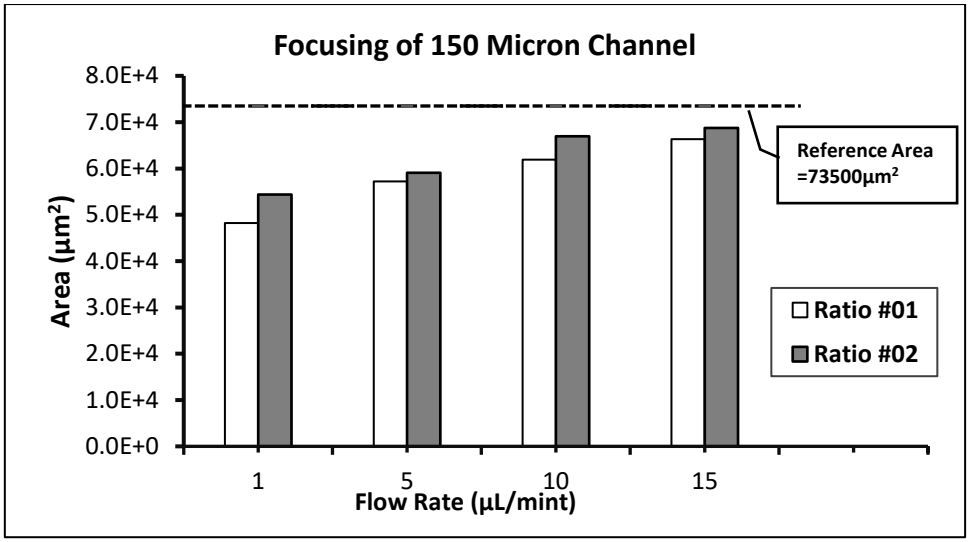

Figure 32 Focusing in 150-micron Channel.

The graph shows the relationship between the flow rate and the focusing of particles in a 150-micron channel. The x-axis represents the flow rate, and the y-axis represents the degree of focusing. The data points on the graph represent the two different particle sizes, with one set of data points representing particles that are 9 microns in size and another set representing particles that are 15 microns in size.

As the flow rate increases, the data points for both particle sizes move upward on the y-axis, indicating that the degree of focusing also increases. This means that as the flow rate increases, the particles tend to become more concentrated in a specific area, or "focused," within the channel.

Furthermore, it can be seen that the data points for the 15-micron particles are higher on the y-axis than the data points for the 9-micron particles at any given flow rate. This illustrates that the degree of focusing is dependent on the size of the particles; larger particles exhibit greater focusing than smaller particles at the same flow rate.

In conclusion, the graph shows that as flow rate increases, the particles in the channel become more focused and that the degree of focusing is greater for larger particles than for smaller particles.

CHAPTER 6 .

CONCLUSION AND FUTURE RECOMMENDATIONS

6.1 Conclusion

In this research, we proposed a cost-effective microfluidics device for blood counting. The device is a time-saving method for counting particles or cells. One of the key features of the device is that it can detect multi-size particles or cells. The experiment was conducted with different flow rates, and the results showed that the flow rate of 1 µL/mint gave the maximum count for both particle sizes. Additionally, the results showed that the smaller the channel size, the higher the counting. For example, the 150-micron channel size had a higher counting rate compared to the larger channel sizes. It is also important to note that the counting result also depends on the device used for the count. In this case, the device used was a microscope camera with a specific lens magnification. By using the ImageJ software to process the images, the particle count was obtained.

The results of our study indicate that the focusing of particles in the 150-micron channel is directly affected by the flow rate. The best focusing was achieved at the highest flow rate of 15µL/mint. Additionally, the focusing also depends on the ratio and size of the particles. It was observed that the higher the particle size, the more focused the stream of particles. Specifically, a ratio of 2 where the number of 15-micron particles is greater resulted in the highest level of focusing. This is due to the presence of 15-micron particles. To achieve the best focusing in a microchannel, the 150-micron channel should be used with the flow rate set to the maximum. However, it should be noted that while particles can still be focused at a flow rate of 1µL/mint, this is not the maximum.

6.2 Future Recommendations

Some future recommendations for further improvement of the microfluidic device for blood counting are:

- The use of more advanced imaging techniques such as high-resolution microscopy and fluorescence imaging to enhance the accuracy of cell counting.
- The incorporation of automated particle counting algorithms to improve the speed and efficiency of the counting process.
- The use of different types of microfluidic devices such as flow-focusing devices and dielectrophoretic-based devices to further improve the separation and concentration of cells.

- The integration of additional functionalities such as cell lysis and sample preparation to the device to allow for on-chip analysis.
- The development of portable and low-cost microfluidic devices for point-of-care applications, which can be used in resource-limited settings.
- The use of microfluidic devices for other types of particles or cells, such as bacteria, viruses, or cancer cells, to extend the range of applications for the device.
- Using the device for monitoring or measuring the properties of the particles such as size, volume, shape and also the concentration of the particles.
- Further studies in terms of the robustness and reproducibility of the device, as well as the evaluation of its performance in real-world samples.

Appendix A

a) b)

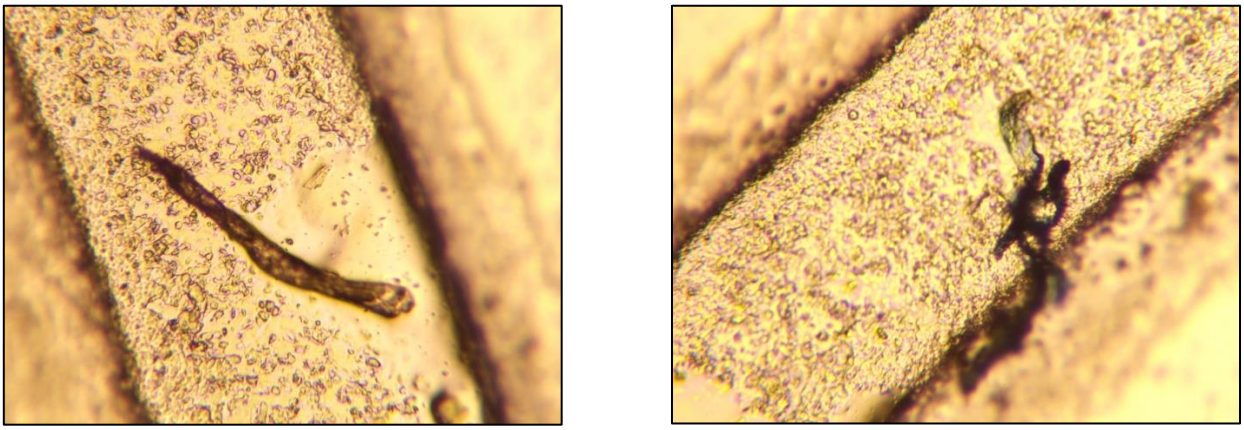

Figure 33 Errors on Channels

a) b)

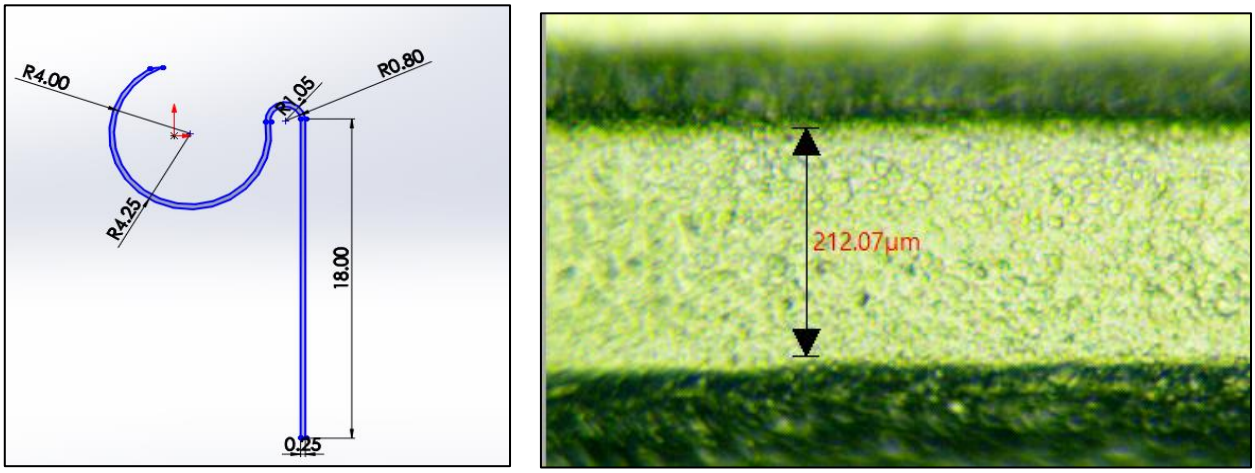

Figure 34 Channel Dimension (dimensions in mm (a) figure)

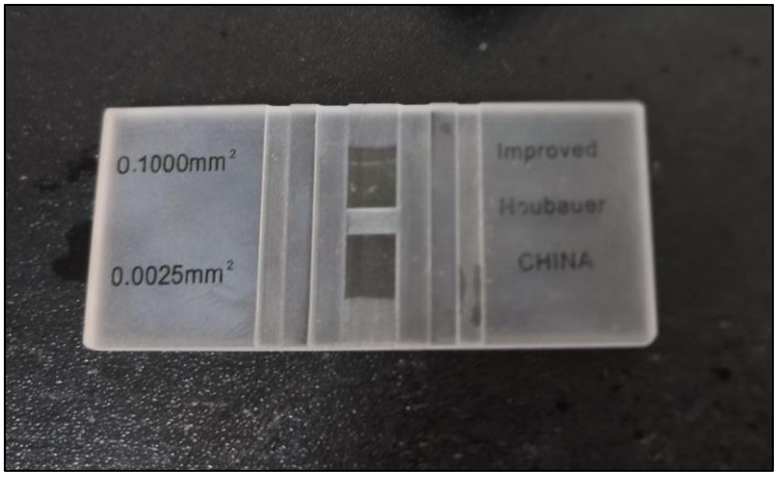

Figure 35 Hemocytometer used for validation

REFERENECS

[1] H. K. Ra, H. Kim, H. J. Yoon, S. H. Son, T. Park, and S. Moon, "A robust cell counting approach based on a normalized 2D cross-correlation scheme for in-line holographic images," *Lab Chip*, vol. 13, no. 17, pp. 3398–3409, Sep. 2013, doi: 10.1039/c3lc50535a.

[2] R. Kishor *et al.*, "Real time size-dependent particle segregation and quantitative detection in a surface acoustic wave-photoacoustic integrated microfluidic system," *Sens Actuators B Chem*, vol. 252, pp. 568–576, 2017, doi: 10.1016/j.snb.2017.06.006.

[3] J. Luo, C. Chen, and Q. Li, "White blood cell counting at point-of-care testing: A review," *Electrophoresis*, vol. 41, no. 16–17. Wiley-VCH Verlag, pp. 1450–1468, Sep. 01, 2020. doi: 10.1002/elps.202000029.

[4] R. Online *et al.*, "Fundamentals and applications of inertial microfluidics: A review Publication Details Fundamentals and applications of inertial microfluidics: A review. Lab on a Chip: miniaturisation for chemistry Fundamentals and applications of inertial microfluidics: A review Publication Details Fundamentals and applications of inertial microfluidics: A review. Lab on a Chip: miniaturisation for chemistry Fundamentals and Applications of Inertial Microfluidics: A Review," 2016. [Online]. Available: http://ro.uow.edu.au/eispapers/4850

[5] "Microfluidic Devices Based on Biomechanics," in *Integrated Nano-Biomechanics*, Elsevier, 2018, pp. 217–263. doi: 10.1016/b978-0-323-38944-0.00007-3.

[6] B. K. Ashley and U. Hassan, "Time-domain signal averaging to improve microparticles detection and enumeration accuracy in a microfluidic impedance cytometer," *Biotechnol Bioeng*, vol. 118, no. 11, pp. 4428–4440, Nov. 2021, doi: 10.1002/bit.27910.

[7] Z. Zhu, X. Xu, L. Fang, D. Pan, and Q. A. Huang, "Investigation of geometry-dependent sensing characteristics of microfluidic electrical impedance spectroscopy through modeling and simulation," *Sens Actuators B Chem*, vol. 235, pp. 515–524, 2016, doi: 10.1016/j.snb.2016.05.092.

[8] Y. Temiz and E. Delamarche, "Sub-nanoliter, real-time flow monitoring in microfluidic chips using a portable device and smartphone," *Sci Rep*, vol. 8, no. 1, Dec. 2018, doi: 10.1038/s41598-018-28983-w.

[9] E. Valera *et al.*, "A microfluidic biochip platform for electrical quantification of proteins," *Lab Chip*, vol. 18, no. 10, pp. 1461–1470, May 2018, doi: 10.1039/c8lc00033f.

[10] A. Farooq, N. Z. Butt, and U. Hassan, “Circular shaped microelectrodes for single cell electrical measurements for lab-on-a-chip applications,” *Biomed Microdevices*, vol. 23, no. 3, Sep. 2021, doi: 10.1007/s10544-021-00574-z.

[11] A. Farooq, N. Z. Butt, and U. Hassan, “Biochip with multi-planar electrodes geometry for differentiation of non-spherical bioparticles in a microchannel,” *Sci Rep*, vol. 11, no. 1, Dec. 2021, doi: 10.1038/s41598-021-91109-2.

[12] J. Berger *et al.*, “Simultaneous electrical detection of IL-6 and PCT using a microfluidic biochip platform,” *Biomed Microdevices*, vol. 22, no. 2, Jun. 2020, doi: 10.1007/s10544-020-00492-6.

[13] C. H. Clausen, G. E. Skands, C. V. Bertelsen, and W. E. Svendsen, “Coplanar electrode layout optimized for increased sensitivity for electrical impedance spectroscopy,” *Micromachines (Basel)*, vol. 6, no. 1, pp. 110–120, 2015, doi: 10.3390/mi6010110.

[14] M. Asraf Mansor and M. Ridzuan Ahmad, “Microfluidic Device for Single Cell Impedance Characterization,” in *Current and Future Aspects of Nanomedicine*, IntechOpen, 2020. doi: 10.5772/intechopen.90657.

[15] M. F. Abdullah, P. L. Leow, M. A. A. Razak, and F. K. C. Harun, “On-Chip Droplets Sensing using Capacitive Technique,” 2012, [Online]. Available: www.jurnalteknologi.utm.my

[16] H. Seto *et al.*, “Development of microparticle counting sensor based on structural and spectroscopic properties of metal mesh device,” *Advanced Powder Technology*, vol. 32, no. 6, pp. 1920–1926, Jun. 2021, doi: 10.1016/j.apt.2021.04.002.

[17] T. Saeki, M. Hosokawa, T. K. Lim, M. Harada, T. Matsunaga, and T. Tanaka, “Digital cell counting device integrated with a single-cell array,” *PLoS One*, vol. 9, no. 2, Feb. 2014, doi: 10.1371/journal.pone.0089011.

[18] Y. H. Lin and G. bin Lee, “Optically induced flow cytometry for continuous microparticle counting and sorting,” *Biosens Bioelectron*, vol. 24, no. 4, pp. 572–578, Dec. 2008, doi: 10.1016/j.bios.2008.06.008.

[19] J. Luo, C. Chen, and Q. Li, “White blood cell counting at point-of-care testing: A review,” *Electrophoresis*, vol. 41, no. 16–17. Wiley-VCH Verlag, pp. 1450–1468, Sep. 01, 2020. doi: 10.1002/elps.202000029.

[20] E. M. Strohm *et al.*, “Sizing biological cells using a microfluidic acoustic flow cytometer,” *Sci Rep*, vol. 9, no. 1, Dec. 2019, doi: 10.1038/s41598-019-40895-x.

[21] Z. J. Smith *et al.*, “Single-step preparation and image-based counting of minute volumes of human blood,” *Lab Chip*, vol. 14, no. 16, pp. 3029–3036, Aug. 2014, doi: 10.1039/c4lc00567h.

[22] J. Zhang *et al.*, “Fundamentals and applications of inertial microfluidics: A review,” *Lab on a Chip*, vol. 16, no. 1. Royal Society of Chemistry, pp. 10–34, 2016. doi: 10.1039/c5lc01159k.

[23] Y. C. Kung, K. W. Huang, W. Chong, and P. Y. Chiou, “Tunnel Dielectrophoresis for Tunable, Single-Stream Cell Focusing in Physiological Buffers in High-Speed Microfluidic Flows,” *Small*, vol. 12, no. 32, pp. 4343–4348, Aug. 2016, doi: 10.1002/smll.201600996.

[24] X. Lu, L. Zhu, R. mao Hua, and X. Xuan, “Continuous sheath-free separation of particles by shape in viscoelastic fluids,” *Appl Phys Lett*, vol. 107, no. 26, Dec. 2015, doi: 10.1063/1.4939267.

[25] J.-A. Kim, J.-R. Lee, T.-J. Je, E.-C. Jeon, and W. Lee, “Supporting Information Size-dependent inertial focusing position shift and particle separations in triangular microchannels.”

[26] J. Takagi, M. Yamada, M. Yasuda, and M. Seki, “Continuous particle separation in a microchannel having asymmetrically arranged multiple branches,” *Lab Chip*, vol. 5, no. 7, pp. 778–784, 2005, doi: 10.1039/b501885d.

[27] H. Amini, W. Lee, and D. di Carlo, “Inertial microfluidic physics,” *Lab on a Chip*, vol. 14, no. 15. Royal Society of Chemistry, pp. 2739–2761, Aug. 07, 2014. doi: 10.1039/c4lc00128a.

[28] D. Tang, L. Jiang, W. Tang, N. Xiang, and Z. Ni, “Cost-effective portable microfluidic impedance cytometer for broadband impedance cell analysis based on viscoelastic focusing,” *Talanta*, vol. 242, p. 123274, May 2022, doi: 10.1016/J.TALANTA.2022.123274.

[29] Y. Wang and X. Guo, “A low-cost and simple on-chip cell counting device based on lensless imaging technology,” in *2022 3rd International Conference on Computer Vision, Image and Deep Learning and International Conference on Computer Engineering and Applications, CVIDL and ICCEA 2022*, 2022, pp. 559–562. doi: 10.1109/CVIDLICCEA56201.2022.9825217.

[30] D. di Carlo, “Inertial microfluidics,” *Lab on a Chip*, vol. 9, no. 21. Royal Society of Chemistry, pp. 3038–3046, 2009. doi: 10.1039/b912547g.

[31] M. Villegas, Z. Cetinic, A. Shakeri, and T. F. Didar, “Fabricating smooth PDMS microfluidic channels from low-resolution 3D printed molds using an omniphobic lubricant-infused coating,” *Anal Chim Acta*, vol. 1000, pp. 248–255, Feb. 2018, doi: 10.1016/j.aca.2017.11.063.

[32] R. Natu, S. Guha, S. A. R. Dibaji, and L. Herbertson, “Assessment of flow through microchannels for inertia-based sorting: Steps toward microfluidic medical devices,” *Micromachines (Basel)*, vol. 11, no. 10, Oct. 2020, doi: 10.3390/mi11100886.

MS Thesis

ORIGINALITY REPORT

5%	4%	1%	3%
SIMILARITY INDEX	INTERNET SOURCES	PUBLICATIONS	STUDENT PAPERS

PRIMARY SOURCES

1	Submitted to Higher Education Commission Pakistan Student Paper	1%
2	Submitted to The Manchester College Student Paper	<1%
3	core.ac.uk Internet Source	<1%
4	Submitted to DeVry, Inc. Student Paper	<1%
5	Submitted to University of Glasgow Student Paper	<1%
6	Misra, Soumyadeep, Linwei Yu, Wanghua Chen, Martin Foldyna, and Pere Roca i Cabarrocas. "A review on plasma-assisted VLS synthesis of silicon nanowires and radial junction solar cells", Journal of Physics D Applied Physics, 2014. Publication	<1%
7	jopss.jaea.go.jp Internet Source	<1%

8	Submitted to Athlone Institute of Technology Student Paper	<1 %
9	gb.education.com Internet Source	<1 %
10	scholarworks.unist.ac.kr Internet Source	<1 %
11	Submitted to De Montfort University Student Paper	<1 %
12	Submitted to Imperial College of Science, Technology and Medicine Student Paper	<1 %
13	open.library.ubc.ca Internet Source	<1 %
14	ulspace.ul.ac.za Internet Source	<1 %
15	uvadoc.uva.es Internet Source	<1 %
16	www.premium-cola.de Internet Source	<1 %
17	discovery.ucl.ac.uk Internet Source	<1 %
18	pdfcoffee.com Internet Source	<1 %
19	journals.jsap.jp Internet Source	

<1%

Exclude quotes	On	Exclude matches	Off
Exclude bibliography	On		